Geomagnetic Storm Impacts on Communication, Navigation, Surveillance, and Air Traffic Management (CNS/ATM)

Abdallah Ahmed Eid

Cairo University

ABSTRACT

On 17 March, and 23 June 2015 secondary Air Traffic Control (ATC) radar was strongly disturbed in Cairo Air Navigation Center (CANC) with deterioration and interruptions of communications (Di) at Cairo international airport the disturbances occurred when the radar antennas were pointing at the Sun. In this paper, we are studying the impacts of geomagnetic storms on Communication, Navigation, Surveillance, and Air Traffic Management (CNS/ATM) by researching and analyzing the number of hours in a geomagnetic storm per year.

According to Dst (<-50 nt) in the period from 2015 to 2021 has been analyzed, associated with (Dst) less than (-50 nT), using Dst records that tabulate the amount and vigor of geomagnetic storms, Sunspot Number (SSN) it is period connects the end of the solar cycle 24 and the beginning of the cycle 25 With comparison the deterioration and interruptions of communications (Di) at Cairo international airport Geomagnetic Storm events occur when the Sun causes disruptions to aviation Communications, Navigation, and Surveillance (CNS) systems, and elevates radiation dose levels at flight altitudes.

Keywords: geomagnetic storms/ sunspot number (SSN)/communications, navigation, surveillance (CNS) and satellite solar outage.

Classification: DDC Code: 621.3848 LCC Code: TK6592.S95

Language: English

London Journals Press

LJP Copyright ID: 392921
Print ISSN: 2631-8474
Online ISSN: 2631-8482

London Journal of Engineering Research

Volume 22 | Issue 8 | Compilation 1.0

Geomagnetic Storm Impacts on Communication, Navigation, Surveillance, and Air Traffic Management (CNS/ATM)

Abdallah Ahmed Eid

ABSTRACT

On 17 March, and 23 June 2015 secondary Air Traffic Control (ATC) radar was strongly disturbed in Cairo Air Navigation Center (CANC) with deterioration and interruptions of communications (Di) at Cairo international airport the disturbances occurred when the radar antennas were pointing at the Sun. In this paper, we are studying the impacts of geomagnetic storms on Communication, Navigation, Surveillance, and Air Traffic Management (CNS/ATM) by researching and analyzing the number of hours in a geomagnetic storm per year.

According to Dst (<-50 nt) in the period from 2015 to 2021 has been analyzed, associated with (Dst) less than (-50 nT), using Dst records that tabulate the amount and vigor of geomagnetic storms, Sunspot Number (SSN) it is period connects the end of the solar cycle 24 and the beginning of the cycle 25 With comparison the deterioration and interruptions of communications (Di) at Cairo international airport Geomagnetic Storm events occur when the Sun causes disruptions to aviation Communications, Navigation, and Surveillance (CNS) systems, and elevates radiation dose levels at flight altitudes. Space weather events may occur on short time scales, with the effects occurring from seemingly instantaneous to a few days hence. The effects of space weather come from processes that are invisible to the human eye. The sole exceptions are the brilliant auroras, spawned by energetic electrons and ions.

Energized auroras indicate the deposition of energy into the upper atmosphere, and may herald the degradation of communications, navigation, and surveillance of aircraft in the vicinity. Therefore, decision- makers in the field of aviation should be aware that the phenomena of space weather can pose a threat to the safety and efficiency of flight operations, as the answer is to know what the effects are, the potential and consequent risks of electromagnetic storms, and the options available to mitigate those risks. This means following aviation regulations, operational rules, and business practices applicable in this field.

Keywords: geomagnetic storms/ sunspot number (SSN)/communications, navigation, surveillance (CNS) and satellite solar outage.

Author: Air Traffic Controller at The National Air Navigation Services Company (NANSC), Cairo, Egypt. MSc of Astrophysics, Astronomy, Space Science and Meteorology Dept., Faculty of Science, Cairo University, Egypt.

I. INTRODUCTION

These solar events and variations can give rise to the following effects aurora, ionospheric disturbances, Solar Particle Events (SPEs), and geomagnetic storms. Probably the most well-known effect of solar-induced geomagnetic storms is the aurora borealis (northern lights) and aurora austral (southern lights). Aurorae begin between 60° and 80° latitude. As a storm intensifies, the aurorae spread toward the equator. During an unusually large storm in 1909, an aurora was visible in Singapore, on the geomagnetic equator. The aurorae provide pretty displays, but they are just a visible sign of atmospheric changes that may wreak havoc on technological systems. The bursts of electromagnetic radiation (ultraviolet and x-ray) from a solar flare journey at the speed of light and

London Journal of Engineering Research

arrive at Earth just 8 minutes after leaving the flare site. Unaffected by the Earth's magnetic field, these emissions directly affect the upper atmosphere (becoming significant below 100km) by producing a temporary increase in ionisation in the sunlit hemisphere of minutes to hours duration called a "sudden ionospheric disturbance" Certain major solar flares and CMEs can shower the Earth, within 30 minutes, with energetic particles (primarily protons).

In this case, the Earth's magnetic field does offer some protection, but some of these particles spiral down the field lines, entering the upper atmosphere in the Polar Regions where they produce additional ionisation in the ionosphere and below. Very energetic and intense events can also lead to increases at lower latitudes. One to four days after a major solar disturbance occurs, a slower cloud of solar material and magnetic field reaches Earth, buffeting the magnetosphere and resulting in a geomagnetic storm.

The bi-polar magnetic field of the Earth points north but the field contained within the material expelled from the Sun can point in any direction.

When the field is orientated in the opposite direction to that of the Earth's, the two magnetic systems interact and the solar material can enter the Earth's magnetosphere. These interactions can produce very large electrical currents, of up to a million amperes, flowing through the ionosphere and magnetosphere, which can change the direction of the Earth's magnetic field at the surface by up to 1 or 2 degrees, mainly in the aurorally regions. (Space Weather effects on airline operations (Captain Bryn Jones, VAA Cosmic Radiation Project Manager), n.d.)

Space weather is driven by the Sun and follows the "solar cycle" closely. This cycle is typically about 11 years in duration and is manifest in many of the irradiative and magnetic properties of the Sun. The solar cycle is defined in terms of "sunspots" on the solar disc. Sunspots are regions of extremely intense localized magnetic fields, which appear darker than the surrounding surface. A sunspot region on the solar surface is akin to an extreme low-pressure system or cyclone on Earth with intense magnetic fields rather than extreme winds. At times, sunspots are rare and the solar disc appears almost without blemish. This occurs at the solar minimum, the start of a solar cycle. Later, sunspots become common and it is normal to see numerous large sunspots, often assembled in complex groups, spread across the solar disc. The peak of the solar cycle, when sunspots are most numerous, is known as the solar maximum. There is a standardized way of counting sunspots present on the solar disc, to give the sunspot number or SSN, which is the traditional indicator of solar activity and the progress of the solar cycle. (Penza et al., 2021)Severe space weather conditions affect the performance of numerous modern technical systems, causing problems not only for national and global economies but for everyday life as well.

Satellite navigation systems are particularly vulnerable, even though systematic monitoring of space weather in general, is still performed on a global scale. Space weather effect correction models applied within the standard satellite positioning service are not capable of tackling the effects of severe space weather conditions and local ionospheric characteristics. Severe space weather effects on the GPS ionospheric delay are intensely studied to provide advanced models of the space weather effects on GPS positioning performance. Here one study of severe space weather conditions and their consequences on the GPS ionospheric delay in Croatia is presented.

The study takes advantage of the availability of the space weather indices and the GPS pseudo-range measurements (taken at the reference site at Osijek, Croatia) related to a major severe space weather event lasting from early October 2003 to late November 2003. (Filjar, 2007)

Space weather impacts occur to communications, navigation, surveillance, radiation-sensitive electronics, and human exposure the system impacts may include: (ICAO, n.d.)

1.1 Unexpected Loss of Communications

— HF voice and HF data link, i.e. Controller Pilot Data Link Communication (CPDLC), on routes where HF is employed;

— Poor or unusable performance of L-band SATCOM;

1.2 Degraded Performance of Navigation and Surveillance That Rely on GNSS

— Automatic Dependent Surveillance- Broadcast (ADS-B) and/or Automatic Dependent Surveillance –Contract (ADS-C) anomalies;
— Sporadic loss-of-lock of GNSS, especially near the equator, post-sunset;

1.3 Unanticipated Non-Standard Performance of On-Board Electronics, Resulting in Reboots and Anomalies; and

1.4 Issues Related to Radiation Exposure by Aircrew and Passengers

II. METHODOLOGY

Identify and manage the risks that threaten the management of air traffic by responding quickly and positively to mitigate the effects of electromagnetic storms that cause disruption and deterioration of communication, navigation, and Surveillance based on satellites (CNS).

Therefore, the researcher believes that the strategic objective of the research is an investigation of:

1) *Safety by:* enhancing global civil aviation safety
2) *Security by:* enhancing the security of the Air Traffic Management (ATM)
3) *Efficiency by:* enhancing Air Traffic Flow Management (ATFM)
4) *Continuity by:* maintaining the continuity of flight operations

Space weather events impact aviation operations by degrading the performance of Communication, Navigation, and Surveillance services and solar radiation can be detrimental to the health of crews and passengers. (ICAO, n.d.) Communication and Navigation satellites can be disabled by significant solar events and more commonly, in the Polar Regions; space weather conditions can blackout high-frequency satellite communication and satellite navigation services for periods from minutes to several hours. (www.ICAO.int, n.d.)

2.1 Space Weather Impacts on Communications

All communications with aircraft EN Route poleward of 82-degree latitude can be lost during a disruptive space weather event. As flight paths venture to the poleward side of the 80th parallel, they lose their communication link with the geosynchronous communication satellites due to the earth's curvature, and conventional HF radio communication must be employed. Solar storms can render HF communications inoperable for periods of minutes to hours over several days during disruptions in the ionosphere's electron density to the point of becoming unable to bounce radio signals back to the aircraft. These disruptions are driven by the size and location of the disturbance on the sun that triggers these events. There are polar-orbiting satellites available to partially fill this communication gap, but to date; most airlines are not equipped to take advantage of this capability. Space weather interferes with HF or VHF/UHF communications, the problems can quickly become serious. No ground-based air traffic control radar is available over the poles or oceans, so without communications, air traffic controllers have no position reports on the plane. (kejian1.cmatc.cn, n.d.)

This means they cannot verify aircraft separation, which compromises the critical Situational awareness needed for flight safety. Furthermore, without a means of contacting the crew, ATC has no way of finding out whether deviations from the flight path have occurred. Ultimately, failure to make contact can result in ATC initiating search and rescue operations.

2.1.1 Communications Issues Related to Recent Space Weather Events are Reported Below:

A. Thirteen overdue position reports for flights over Central East Pacific and Central West Pacific (1830-1930Z Jan 27, 2012, R3 radio blackout)
B. HF service degraded for over two hours (Oct 19, 2003, R3 radio blackout)

C. Degradation of high latitude (Oct 24, 2003, G3 geomagnetic storm)
D. Widespread HF communications problems in Alaska (Jan 22-23, 2012 S3 SRS)
E. Communications problems in Asia and the Pacific (Jan 22, 2012, daytime R2 radio blackout)
F. Communications problems off U.S. East Coast and West Coast (Jan 27, 2012 daytime radio blackout)

2.2 Space Weather Impacts on Satellite Navigation

Geomagnetic Storms: Disturbances in the geomagnetic field caused by gusts in the solar wind that blows by Earth. Typical effects from geomagnetic storms include degradation of HF radio transmissions, satellite navigation degradation, and disruption of low-frequency radio navigation systems. (Fisher and Kunches, 2011) Geomagnetic storms can also disrupt electrical power grids, and GPS operations are susceptible to these power outages. Geomagnetic storms also weaken the ability of the Earth's magnetic field to deflect incoming charged particles.

III. DATA SOURCES

The data used for this study is classified and retrieved with the permission of the Air Traffic Control System (ATCS). Is a device in the French THALES system (Thales Group, n.d.) that identifies errors and threats that affect air traffic management, which is recorded in the air safety department and followed up periodically through the International Civil Aviation Organization to develop and raise efficiency. We have collected the events with the number of hours Dst (<-50nT) during the period 2015–2021. A list of magnetic storms based on the Dst indices provided by Kyoto University's Data Analysis Center for Geomagnetism and Space Magnetism Graduate School of Science (wdc.kugi.kyoto-u.ac.jp, n.d.), the number of days with a geomagnetic storm per year. According to the finalized KP-index GFZ Potsdam periods from 2015 to 2021, the KP index We used the monthly SSN provided by the Solar Influences Data Analysis Center (sidc.oma.be) and the solar polar field throughout the solar sunspot cycle provided by the Wilcox Solar Observatory (wso.stanford.edu, n.d.). The source of the data is taken from (c=AU; co=Commonwealth of Australia; ou= Department of Sustainability, n.d.)

The total sunspot number data is provided by the Royal Observatory of Belgium, Brussels, and can be downloaded from the SILSO website (www.sidc.be, n.d.). In addition, it can be found at (www.ngdc.noaa.gov, n.d.)

IV. RESULTS AND DISCUSSION

We have followed the duration of (*Di*) at (CANC) in the period for study from 2015 to 2021 by monitoring and following up on all the days of the interruption during the previous years It is observed in all the monitoring years (*Di*) from 2015 to 2019 the rise in the (*Di*) is the observed year 2015 and then the gradual decline and disappearance the year 2019 It is noted that the duration of (*Di*) increased in Cairo year 2020 and 2021, the beginning of the index rises again and we noted that communications have been repeatedly deteriorated and interrupted at Cairo Air Navigation Center. The equation (1) below is used to calculate the total duration (*Di*) for every year from 2015 to 2021.

$$D_i = \sum_{j=1}^{k} C_{ij} \qquad i = 1, 2, \cdots, 7 \tag{1}$$

Where D_i , = 1, 2, ···, 7. Is the total duration of the deterioration and interruptions of the communications during a specific year from 2015 to 2021, respectively, and C_{ij}, =1, 2, ···, 7.

j=1, 2, ···, is the duration of the deterioration and interruptions of the communications during the specified year ***i***, and ***k*** refers to the number of days of the specified year.

London Journal of Engineering Research

Table 1: This Shows the Total Number of Deterioration and Interruptions of Communications That Happen Annually in Minutes, Over the Study Period (2015 - 2021) at (CANC)

Year	2015	2016	2017	2018	2019	2020	2021
Duration(MIN)	575	493	380	360	250	355	370

The graph below shows the duration of (*Di*) at (CANC) the maximum in the year 2015 is 575 MIN, and the minimum in the year 2019 is 250 MIN, which indicates the beginning of the index rise again in the year 2020 and 2021.

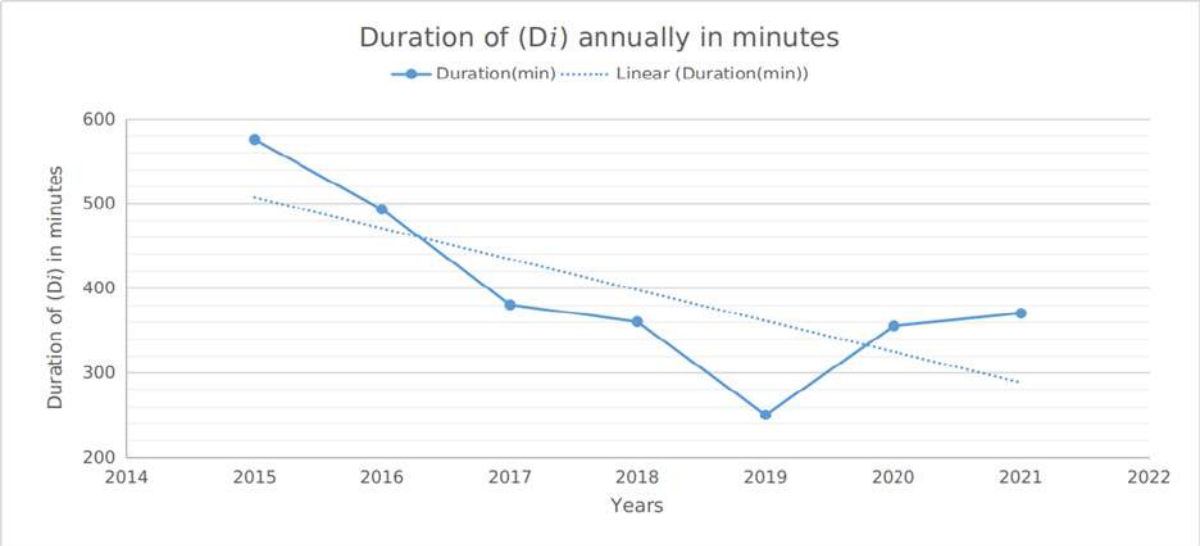

Figure 1: The Duration of (*Di*) at (CANC) in the Periods From 2015 to 2021

4.1 Satellite Solar Outage Impact

The duration of (Di) at (CANC) in the periods from 2015 to 2021 during Satellite Solar Outage It is noted high of the duration of (Di) during Satellite Solar Outage has increased in Cairo in 2015 and gradually decreased until 2020 and indicates the beginning of the index rise again in the year 2021(Guo et al., 2012)

The equation (2) below is used to calculate the total duration (*Di*) during periods I and II for every year from 2015 to 2021

$$D_i = \sum_{j=1}^{m} C_{i1j} + \sum_{j=1}^{n} C_{i2j} \qquad i = 1, 2, \cdots, 7 \tag{2}$$

Where *Di*, $i = 1, 2, \cdots, 7$. is the total duration of the deterioration and interruptions of the communications during a specific year from 2015 to 2021 , respectively *Ci*1*j*, $i = 1, 2, \cdots, 7$,

$j = 1, 2, \cdots, m$ is the duration of the deterioration and interruptions of the communications during the period I in the specified year *i* and *m* refers to the number of days of February and March in the specified year *i*, and *Ci*2*j*, $i = 1, 2, \cdots, 7, j = 1, 2, \cdots,$ *n* is the duration of the deterioration and interruptions of the communications during period II in the specified year *i*, and *n* refers to the number of days of September and October in the specified year *i*. Notated that period I starts from the first day of February till the end day of March in the specified year *i*, while period II starts from the first day of September till the end day of October in the specified year *i*.

Table 2: Shows the total number of deterioration and interruption of communication that happens annually in minutes, to the Satellite Solar Outage (period I and II) (2015-2021)

Year	2015	2016	2017	2018	2019	2020	2021
Duration(min)	434	381	324	294	239	198	240

The graph below shows the duration of (*Di*) at (CANC) in the periods from 2015 to 2021 during Satellite Solar Outage (periods I and II)) the maximum in the year 2015 is 434 MIN, and the minimum in the year 2020 is 198 MIN, which indicates the beginning of the index rise again in the year 2021.

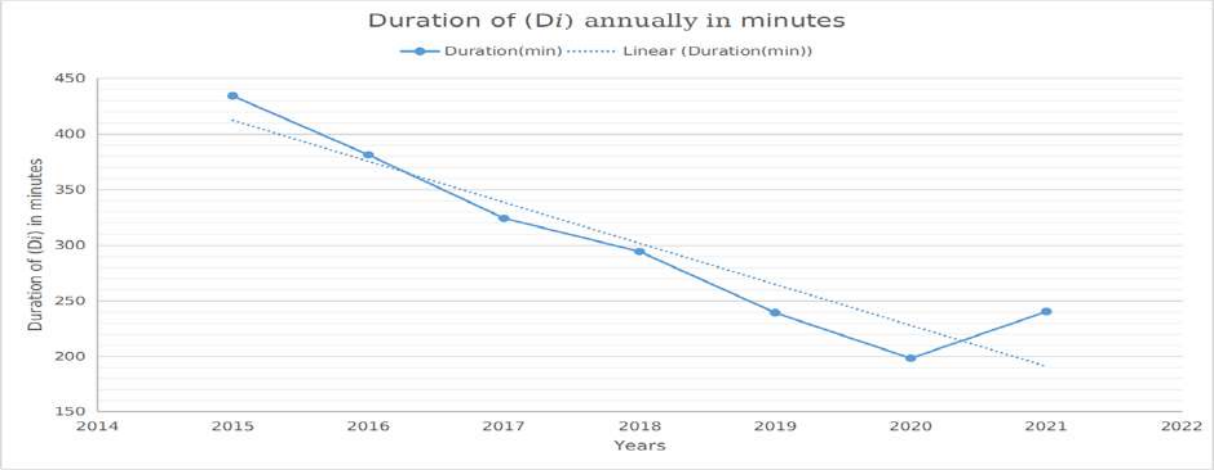

Figure 2: Shows the Duration of (Di) at (CANC) in the Periods From 2015 to 2021 During Satellite Solar Outage (Period I and II)

4.2 Geomagnetic Storms

A geomagnetic storm is a major temporary disturbance in the Earth's magnetic activity and is associated with solar activity, e.g., coronal mass ejection (CME) and high-speed solar wind stream (HSS) (S. O. Ikubanni et al., 2020). When there is greater solar activity, geomagnetic storms are mainly generated by CME; while during moments of less solar activity, it is the coronal holes that have a dominant effect (Gonzalez, Tsurutani, and Clúa de Gonzalez, 1999). Geomagnetic storms occur when there is a large sudden change in the solar wind dynamic pressure at the magnetopause (Mengistu Tsidu and Abraha, 2014)The distinctive characteristic of a geomagnetic storm is a clear decrease in the horizontal intensity of the magnetic field (Gonzalez et al., 1994) Geomagnetic storms can be usually divided into three main phases: initial, main, and recovery (Joshua et al., 2014). Geomagnetic storms are detected prior to the ionospheric disturbances and to the decrease in positioning estimation.

Different geomagnetic indices are used to characterize geomagnetic storms such as the disturbance storm time (Dst) index, geomagnetic disturbance (Kp), averaged geomagnetic activity (Ap) (based on data from a set of specific Kp stations), and the auroral electrojet (AE) index, where the Dst-index is associated with the effects on the equatorial region, the Kp-index to the mid-latitudes, and the AE-index at high latitudes since it characterizes the intensity of ionospheric currents during magnetic storms and substorms activity (Davis and Sugiura, 1966) and (Boroev and Vasiliev, 2020).

The Dst-index has been used historically to characterize the severity of a geomagnetic storm.

Depending on the Dst value, the storms are usually classified in ranges such as weak (−30 nT and −50 nT), moderate (−50 nT and −100 nT), intense (−100 nT and −200 nT), very intense (−200 nT and −350 nT), and great (Dst below

−350 nT) (Borovsky and Shprits, 2017) Furthermore, the Kp-index is based on 3 h measurements from ground- based magnetometers around the world (www.spacew eatherlive.com, n.d.) The storms are usually classified as minor (G1) with a Kp = 5; moderate (G2) with a Kp = 6; strong (G3) with a Kp = 7; severe (G4) with Kp = 8, and extreme (G5) with Kp = 9 (www.swpc.noaa.gov, n.d.).The Ap-index provides a daily average level for geomagnetic activity. The Kp-value converts to a linear scale called the a- index. The average from eight daily a-values gives us the Ap-index of a certain day. Thus, high levels of geomagnetic activity have a higher daily Ap-value (Matzka et al., 2021).

The geomagnetic storms can also be identified by various other parameters such as the symmetric disturbance of the magnetic field H (SYM-H); the interplanetary electric field (IEF); and the interplanetary magnetic field (IMF), where IMF-Bz is the most important parameter for the study of geomagnetic storms, as the energy input into the magnetosphere, depends on Bz orientation and its magnitude (Desai and Shah, 2018) Although these indexes provide extra information regarding the space conditions, some of them are related to The Dst-index. For instance, a relationship has been shown between Dst and Bz (Gonzalez and Echer, 2005). The response of the ionosphere to geomagnetic-induced disturbances is known as an ionospheric storm (Mendillo, 2006) and (Joshua et al., 2018).

The ionosphere plasma density is mainly determined by the chemistry/composition, transport due to electric fields, transport due to neutral wind, and transport due to ambipolar diffusion. During geomagnetic storms, the variations of chemistry or the thermospheric composition, the interaction with the neutrals (neutral wind) (Cai et al., 2021) and (Yu et al., 2021 and/or variations of electric field and ambipolar diffusion (Tsurutani et al., 2008) are the final cause that alters the ionosphere plasma density. Nevertheless, the response of the ionosphere during a geomagnetic storm is complex and difficult to predict accurately, and the physical nature of many underlying mechanisms needs a better understanding to obtain precise forecasting of its behavior based on geomagnetic storm parameters (Samed Inyurt, 2020).

In addition, the effects of these physical processes on the ionosphere have also been reported to vary with solar activity, storm intensity, storm duration, season, location, local time, and altitude of the observing station, which increases the forecast uncertainties (Liu et al., 2008).

The table2: below shows the number of days with a geomagnetic storm per year from 2015 to 2021 and how strong those storms were (www.gfz-potsdam.de, n.d.) during the end of the Solar Cycle 24 and the beginning of the Solar Cycle 25. The Source of the Kp index is the Kp-website of GFZ (www.gfz-potsdam.de, n.d.)

Year	G1	G2	G3	G4	G5	Total
2015	43	18	5	3	0	68 days
2016	45	18	0	0	0	63 days
2017	37	12	2	2	0	53 days
2018	12	7	2	0	0	21 days
2019	16	2	0	0	0	18 days
2020	8	1	0	0	0	9 days
2021	19	4	1	1	0	25 days

Table 2: Shows the Number of Days With a Geomagnetic Storm per Year According to Finalized KP-Index GFZ Potsdam, Over the Study Period (2015-2021)

Year	2015	2016	2017	2018	2019	2020	2021
Number of Day	68	63	53	21	18	9	25

The graph below shows the number of days with a geomagnetic storm per year and how strong those storms were. This will give you an idea of which years there were many geomagnetic storms in the periods from 2015 to 2021. The Source of the Kp index is the Kp-website of GFZ (www.gfz-potsdam.de, n.d.) the maximum in the year 2015 is 68 Days, and the minimum in the year 2020 is 9 days which indicates the beginning of the index rise again in the year 2021.

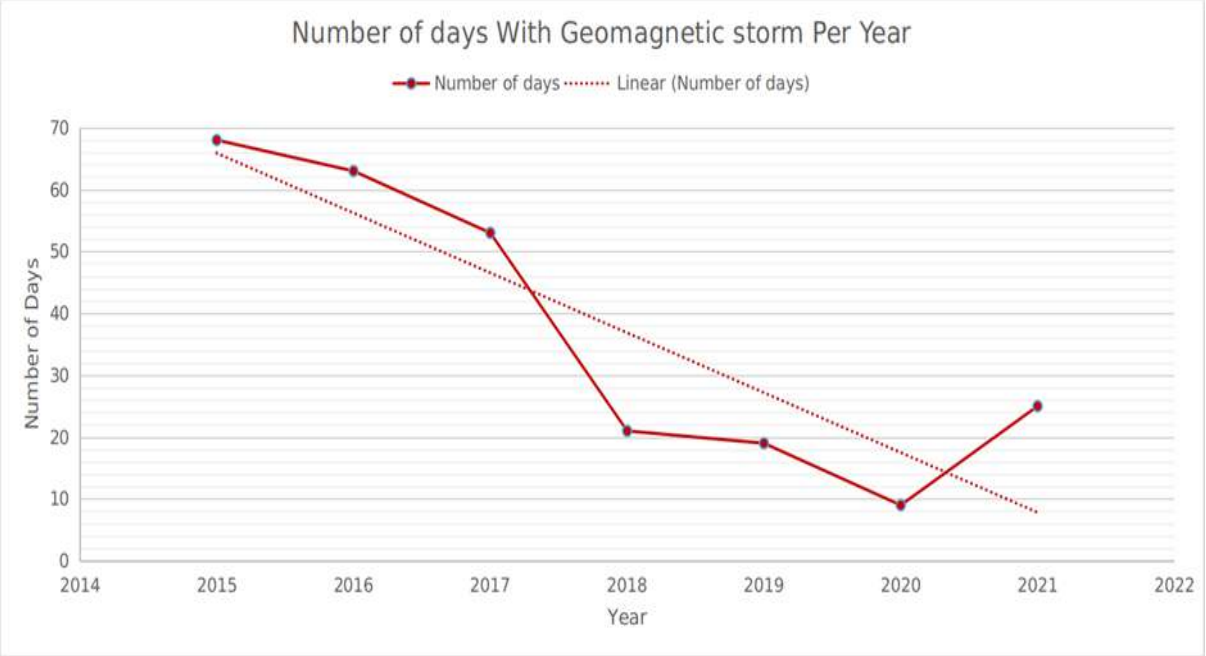

Figure 3: The Number of Days With a Geomagnetic Storm per Year According to Finalized KP- Index GFZ Potsdam Periods From 2015 to 2021

The disturbance storm time (Dst- index) is a measure in the context of space weather. It gives information about the strength of the ring current around Earth caused by solar protons and electrons. The ring current around Earth produces a magnetic field that is directly opposite Earth's magnetic field, i.e. if the difference between solar electrons and protons gets higher, then Earth's magnetic field becomes weaker (Clette et al., 2015). A negative Dst value means that Earth's magnetic field is weakened. This is particularly the case during Geomagnetic storms. (Kyoto-u.ac.jp, 2022)

The Dst-index has been used historically to characterize the severity of a geomagnetic storm. Depending on the Dst value, the storms are usually classified in ranges such as weak (−30 nT and −50 nT), moderate (−50 nT and −100 nT), intense (−100 nT and −200 nT), very intense (−200 nT and −350 nT), and great (Dst below −350 nT), (Borovsky and Shprits, 2017) and Our study will depend on the intensity of the geomagnetic storm. Depending on the value of Dst, storms are classified as moderate (−50 nT) periods from 2015 to 2021 during the end of Solar Cycle 24 and the beginning of Solar Cycle 25.

To get the number of hours with a Geomagnetic Storm per year (N_i), we present the following equation (3)

$$N_i = \sum_{j=1}^{k} G_{ij} \qquad i = 1, 2, \cdots, 7 \tag{3}$$

Where N_i,i=1,2,⋯,7 is the total number of hours with a Geomagnetic Storm during a specific year from 2015 to 2021, respectively and G_{ij}, i=1,2,⋯,7, j =1,2,⋯,k is the number of the hours with a Geomagnetic Storm during the specified year i with, Dst < −50 nt and k refer to the number of days of the specified year i.

The year 2015 was chosen because it is the highest in the number of hours with a geomagnetic storm per year According to Dst (< -50 nt) The period from 2015 to 2021 connects the end of the solar cycle 24 and the beginning of the cycle 25. We have followed the Number of hours with a geomagnetic storm per year According to Dst (< -50 nt) in the period for study from 2015 to 2021 by monitoring and using Equation (2) We found the number of hours with a geomagnetic storm per year According to Dst (< -50 nt) have increased in 2015 and gradually decreased until 2019 and increased during the year 2020 and 2021, i.e. the beginning of the index rise again The graph below shows the number of hours with a Geomagnetic Storm per year According to Dst (< -50 nt) in the period from 2015 to 2021.

Table 4: Shows the Number of Hours With a Geomagnetic Storm per Year According to Dst (< -50 Nt), Over the Study Period (2015-2021)

Year	2015	2016	2017	2018	2019	2020	2021
Number of hours	560	182	89	64	14	25	55

The graph below shows the number of hours with a Geomagnetic Storm per year According to Dst (< -50 nt)in the period from 2015 to 2021, the maximum in the year 2015 is 560 hours, and the minimum in the year 2019 is 14 hours which indicates the beginning of the index rise again in the year 2020 and 2021.

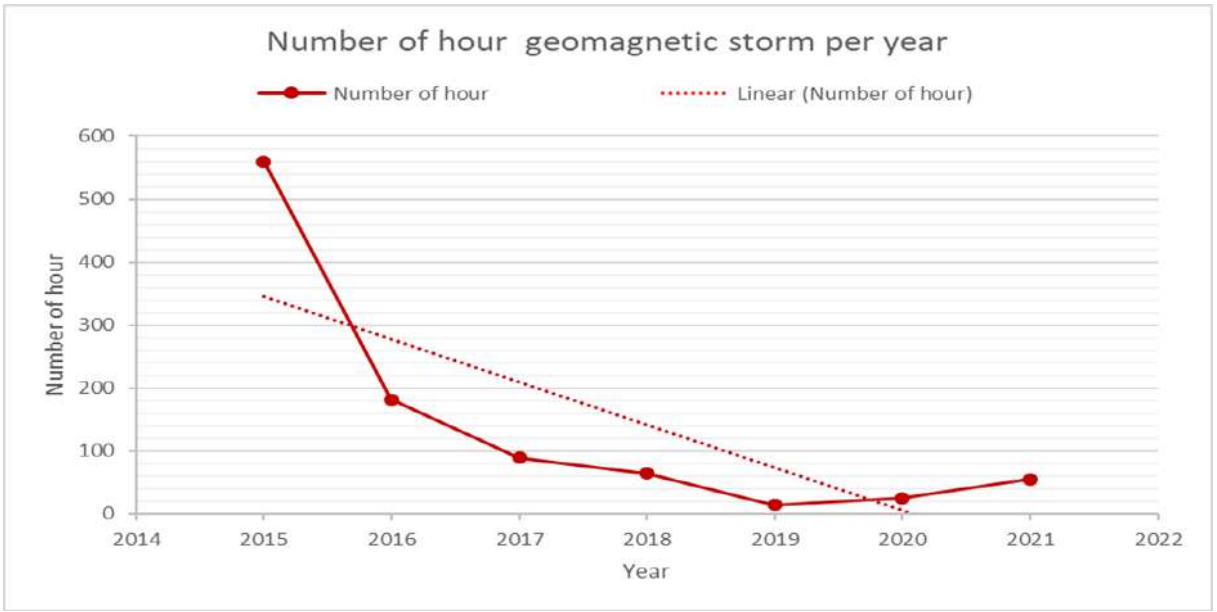

Figure 4: The Number of Hours With a Geomagnetic Storm per Year According to Dst (< -50 Nt) in the Period From 2015 to 2021

4.3 The Solar Cycle and Sunspots

Space weather is driven by the Sun and follows the "solar cycle" closely. This cycle is typically about 11 years in duration and is manifest in many of the irradiative and magnetic properties of the Sun. Solar activity is not constant and, from time to time, eruptions appear on the sun's surface which results in an abnormal level of radiation and particle ejection. (Clette et al., 2015)

The equation (4) below is used to calculate the Observed Sunspot Number (S_i) for every year from 2015 to 2021

$$S_i = \sum_{j=1}^{12} S_{ij} \qquad i = 1, 2, \cdots, 7 \tag{4}$$

Where $S_i, i = 1, 2, \cdots, 7$ the total sunspot numbers during a specific year from 2015 to 2021, respectively, and $S_{ij}, i = 1, 2, \cdots, 7, j = 12, \cdots, 12.$ is the observed monthly sunspot number.

We have followed the Solar Cycles (SSN) in the period for study from 2015 to 2021 by monitoring and using Equation (4) We found the Solar Cycles (SSN) increased in 2015 and gradually decreased until 2019 and increased during the year 2020 and 2021, i.e. the beginning of the (SSN) rise again. The graph below shows sunspot measurements for Solar Cycle 24, which ended in 2019 and started new Solar Cycle 25 in the period from 2015 to 2021

Table 5: Shows the Sunspot Number (SSN), Over the Study Period (2015-2021)

Year	2015	2016	2017	2018	2019	2020	2021
Sunspot Number	783.4	477.9	261.8	84.1	43	105.5	353.8

The graph below shows the Sunspot Number (SSN) in the period from 2015 to 2021 the maximum in the year 2015 is 783.4, and the minimum in the year 2019 is 43, which indicates the beginning of the index rise again in the year 2020 and 2021.

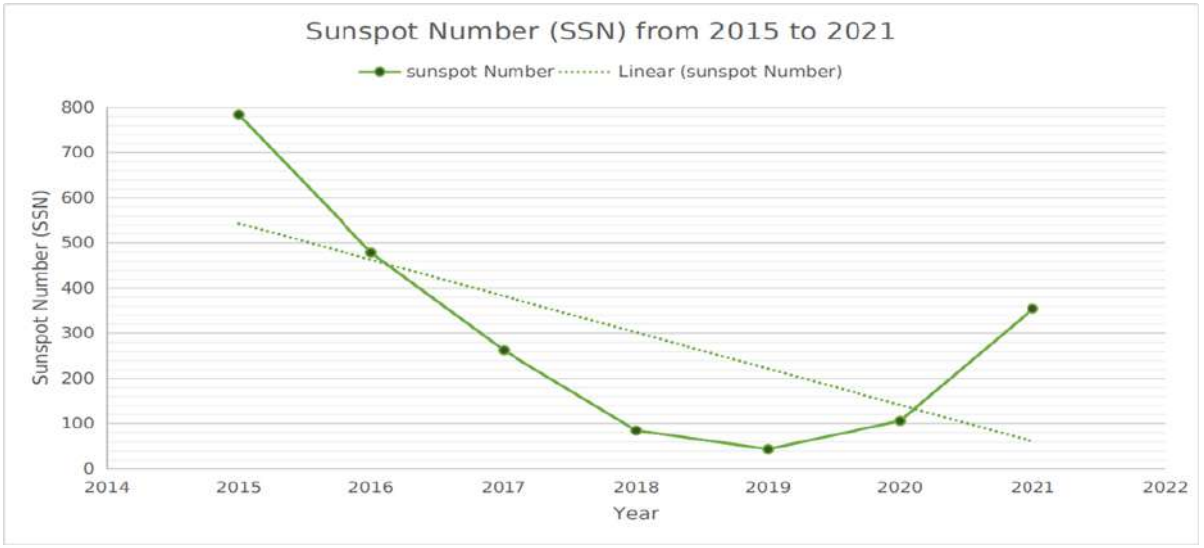

Figure 5: Sunspot Number (SSN) in the Period From 2015 to 2021

Table 6: Shows a Comparison between The number of hours with a geomagnetic storm per year According to Dst (< -50 nt), Sunspot Number (SSN), and the Duration of (*Di*) at (CANC), over the study period (2015-2021) we noticed an increase in 2015 and gradually decreased until 2019 and increased during the year 2020 and 2021, namely the occurrence rate tends to be increased

Year	2015	2016	2017	2018	2019	2020	2021
Dst	560	182	89	64	14	25	55
Sunspot Number	783.8	477.9	261.8	84.1	43	105.5	353.8
Duration	575	493	380	360	250	355	370

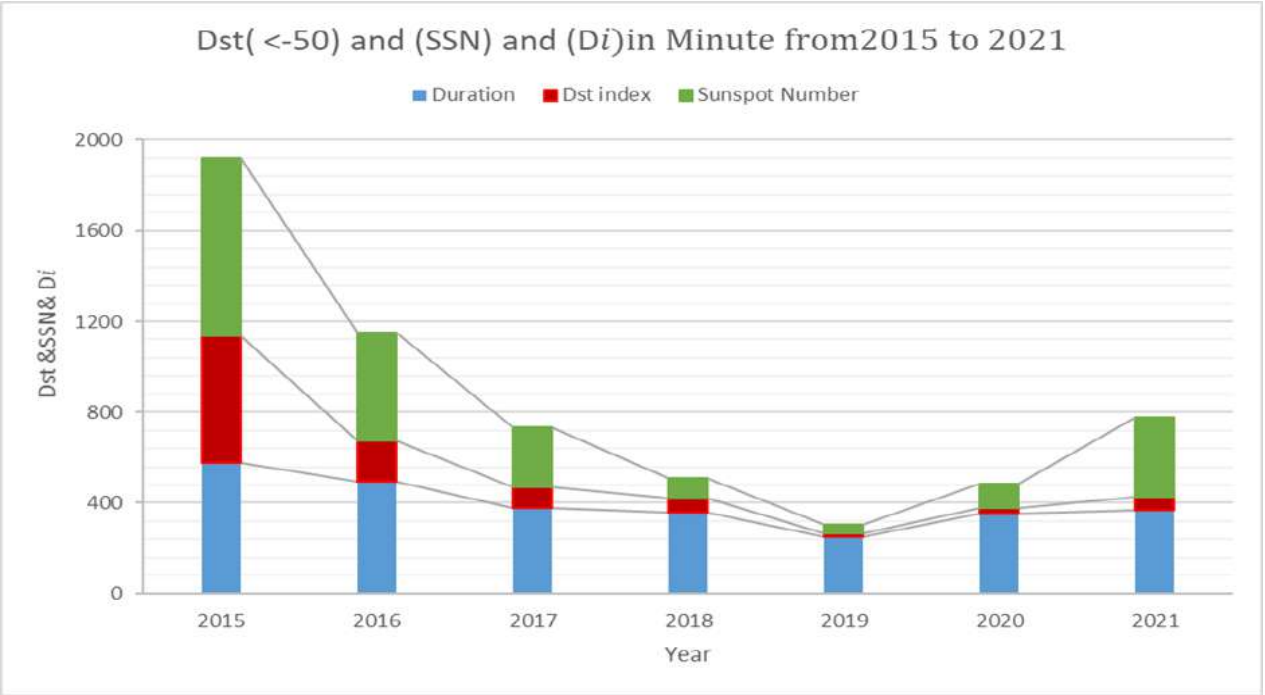

Figure 6: Shows a Comparison Between the Number of Hours With a Geomagnetic Storm per Year According to Dst (< – 50 Nt) and the Solar Cycles (SSN) and the Duration of (Di) at (CANC) in the Period From 2015 to 2021

V. CASE STUDY (1) EVENT OF 17 MARCH 2015 AT CAIRO INTERNATIONAL AIRPORT

On 17 March 2015 at Cairo International airport, radar failure, and loss of radar identification, instructions were issued to restore non-radar standard separation and the pilot was instructed to communicate with the ATS unit concerned.

Therefore, without communications, air traffic controllers have no position reports on the plane.

This means they cannot verify aircraft separation, which compromises the critical situational awareness needed for flight safety.

Furthermore, without a means of contacting the crew, ATC has no way of finding out whether deviations from the flight path have occurred.

Ultimately, failure to make contact can result in ATC initiating search and rescue operations. The (*Di*) is 40 minutes on17 March 2015, the graph below shows the duration of (*Di*) in minutes at Cairo International airport on 17 March 2015.

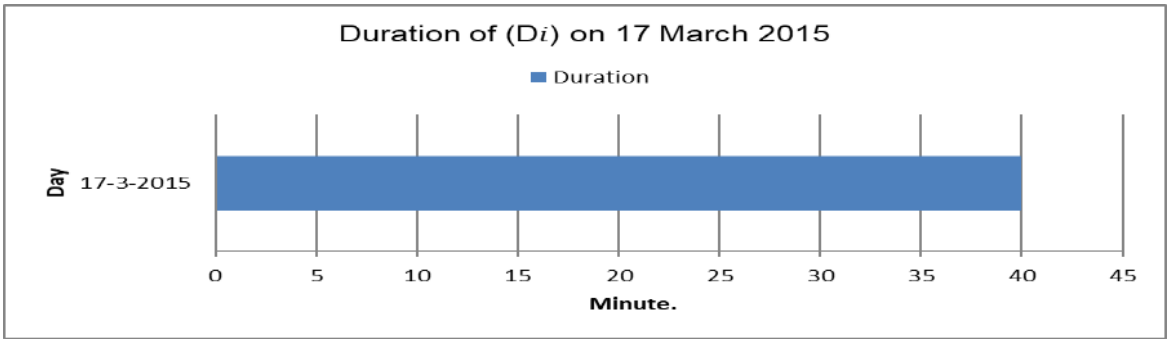

Figure 7: Shows the Duration of (Di) in Minutes at the Cairo International Airport on 17 March 2015

The geomagnetic storm under study occurred on 17 March 2015. It can be classified as The Strongest G4 Storm of Solar Cycle 24, known as the St. Patrick's Day storm on March 17, 2015, Super Geomagnetic Storm (−200 nt) The main phase of this storm lasted two hours or 120 minutes originating by the impact on Earth's atmosphere of coronal mass ejections (CMEs), the storm reaching the condition of G4 (severe) level, in the NOAA geomagnetic scale (Kil et al., 2016) The graph below shows the super geomagnetic storm Dst(< −200 nt) of solar cycle 24 which occurred on 17 March 2015.

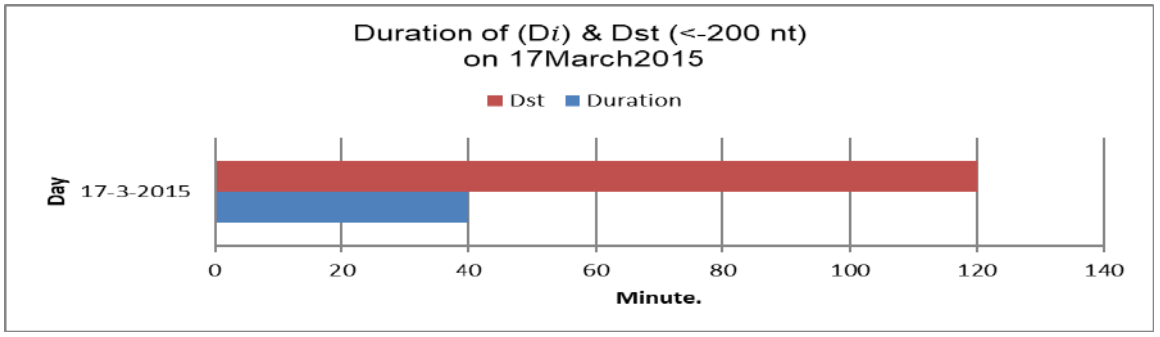

Figure 8: Shows a Comparison Between the First Super Geomagnetic Storm of Solar Cycle 24 Occurred Dst (< −200 nT) and the Duration of (*Di*) at Cairo International Airport on 17 March 2015

VI. CASE STUDY (2) EVENT OF 23 JUNE 2015 AT CAIRO INTERNATIONAL AIRPORT

The graph below shows the deterioration and interruption of communication at Cairo International airport in 25 minutes. This event affected the safety and security of Egyptian Air Traffic Management on 23 June 2015.

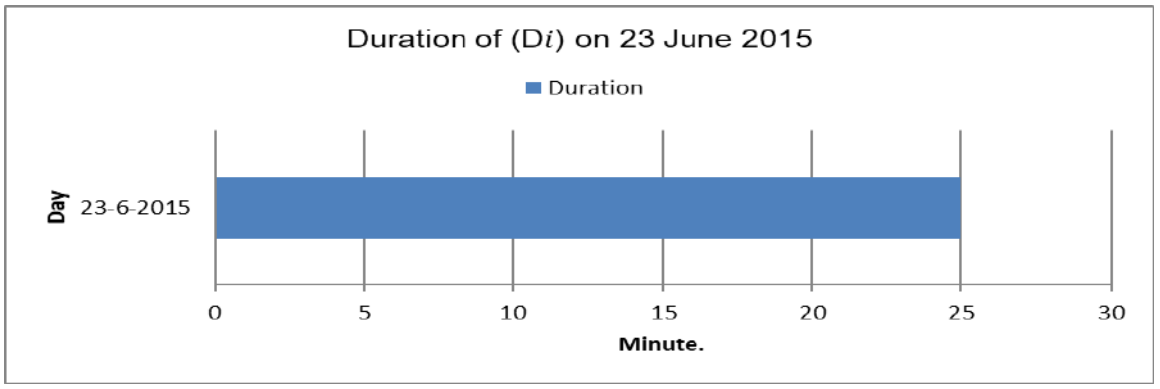

Figure 9: Shows the Duration of (*Di*) at the Cairo International Airport on 23 June 2015

After analyzing the data shown in the graph below Comparison the duration of (*Di*) at Cairo International airport is 25 minutes and The second largest geomagnetic storm Dst (< −200 nt) is 60 minutes on June 23, 2015, we noticed this event has affected the safety and security of Egyptian Air Traffic Management.

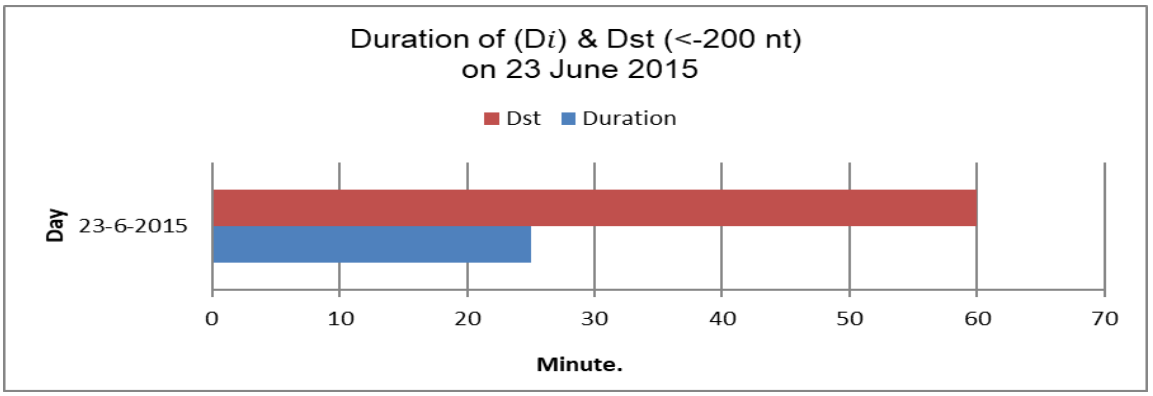

Figure 10: Shows a comparison between Geomagnetic storm Dst (< −200 nT) of Solar Cycle 24 that occurred on 23 JUNE, 2015, and the duration of (*Di*) at the Cairo International airport on June 23, 2015

VII. CONCLUSION

Realize the objective of diagnosing how geomagnetic storms affect CNS/ATM (communication, navigation, surveillance, and air traffic management). According to a study and analysis of the outages and degradation of contacts in the base's air center from 2015 to 2021, the maximum outage and disruption of communications occurred in 2015 for a total of 575 minutes, and the minimum occurred in 2019 for a total of 250 minutes. In 2020, however, the degradation and disruption of communications started to rise once more for a total of 355 minutes, and after monitoring in 2021, it was confirmed that it occurred for 370 minutes.

Aswan International Airport in Egyptian airspace is the change of the natural geographical process of study in general, and the results are identical to those of the first Cairo International Airport, with (*D1*) Act 2015 being 605 minutes, which is the majority, as well as (*D5*) for the year 2019 being 285 minutes, which is the minimum, and the beginning of the increase in (*D6*) 2020 being 375 minutes, which indicates the beginning of the rise. The investigation and analysis of the communications breakdown and deterioration at the Cairo Aeronautical Center during Periods I and II of the Satellite Solar Outage, The conclusion drawn from the two time periods above is that (*D1*) for the year 2015 is the highest degree and (*D6*) for the year 2020 is the lowest

degree. Studying and analyzing how communications in the second terminal of the Aswan International Airport changed and were disrupted during the same two times as above led to the conclusion that (*D1*) for the year 2015 was the highest degree and (*D6*) for the year 2020 was the lowest degree.

Based on research and analysis of the number of geomagnetic storm days per year from 2015 to 2021, the largest number of days, or 68 per day, is categorized as follows:

The minimum number of geomagnetic storm days in a year is specifically one day for which they are classed as follows: 43 days of a minor (G1), 18 days of moderate (G2), 5 days of strong (G3), and 3 days of severe (G4). 1 day of a moderate, 8 days of a minor (G1) (G2).

The duration of a geomagnetic storm in hours per year has been studied and analyzed. In the years 2015 through 2021, the greatest number of hours worked is 560, and the minimum number of hours worked is 14, according to Dst (-50 nt).

Using Dst records that tabulate the quantity and intensity of geomagnetic storms, Sunspot Number (SSN), and the deterioration and interruptions of communications (*Di*), the number of hours of geomagnetic storm per year for the period (2015–2021) has been examined.

This period spans the end of solar cycle 24 and the start of cycle 25, and it is associated with (Dst) less than (-50 nT). Because there are more solar active regions visible during this time, it is thought that the majority of intense geomagnetic storms, communication deterioration, and interruptions happen during the maximum phase of the sunspot. In contrast, only a small number of these events are seen during the minimum phase of the sunspot.

Study and evaluation of the monthly Sunspot Number (SSN) (2015 to 2021). Its maximum value is around 838 in the year 2015, and its smallest value is 43 in the year 2019.

After examining the data, we discovered that there was a 120-minute gap between the time (*Di*) at Cairo International Airport on March 17, 2015, and the Super Geomagnetic Storm Dst (-200 nt), also known as the St. Patrick's Day storm, which was the strongest G4 storm of Solar Cycle 24. This event had an impact on the security and safety of Egyptian Air Traffic Management.

When we compared the duration of the second-largest geomagnetic storm, Dst(-200 nt), on June 23, 2015, to the duration of (*Di*) at Cairo International Airport, which was 25 minutes, we saw that this event had a negative impact on the safety and security of Egyptian Air Traffic Management.

Even in other airports, such as but not limited to Aswan International Airport, after ongoing surveillance and follow-up of this Important in Cairo International Airport On March 17, 2015, the airport experienced the same issue as previously described both at once. After comparing the durations of (*Di*) at Aswan International Airport and the Super Geomagnetic Storm Dst (-200 nt), which is known as St. Patrick's Day and lasts 120 minutes, we observed that this event has had an impact on the safety and security of Egyptian Air Traffic Management on March 17, 2015. After comparing the data, we discovered that on June 23, 2015, this event had a negative impact on the security and safety of Egyptian Air Traffic Management.

The duration of (*Di*) at Aswan International Airport was 33 minutes, while the second-largest geomagnetic storm, Dst (-200 nt), was 60 minutes. The main findings of this study suggest a direct association between the first super geomagnetic storm Dst (-200 nt) of solar cycle 24 that occurred on "St. Patrick's day," March 17, 2015, and (*Di*) at Cairo International Airport on March 17, 2015. Communication, navigation, surveillance, and air traffic control will all suffer when there is a satellite solar outage during periods II, a moderate or violent geomagnetic storm, and I during the sunspot cycle's peak. The answer is to be aware of the effects, the potential and consequent risks of electromagnetic storms, and the options available to mitigate those risks.

As a result, decision-makers in the field of aviation should be aware that space-weather phenomena can pose a threat to the safety and efficiency of flight operations. This entails abiding by the relevant business procedures, operational guidelines, and aviation regulations.

VIII. RECOMMENDATIONS

The Egyptian aviation sector is vulnerable to the impacts of space weather, which can affect High-Frequency radio communication, satellites, avionics, and aircraft navigation and communication systems. Internationally, ICAO is requiring that certain standards be developed to assist aircrew and ground support in managing the potential impact of space weather. The main recommendation from this policy brief is that Cairo Air Navigation Center (CANC) should align itself with international for the provision and access to space weather information to be ready to meet the ICAO recommendations by 2025 and to protect the vulnerable areas within aviation systems.

The following recommendations are put forward within this policy brief for consideration:

- Cairo Air Navigation Center (CANC) user forum, with participation from affected parties within the sector should be established to consider and make provision for space weather impacts on aviation.
- Cairo Air Navigation Center (CANC) should be requested to lead the aviation Community in defining and collecting operational data that can be used to assess the different Impact areas, and the economic impact arising from space weather mitigation.
- The aviation industry, with the assistance of the Space weather monitoring Center (SWMC) in Egypt, should be requested to clearly define its requirements for space weather information and how these can be incorporated into the operational decision-making process.
- The Space weather monitoring Center (SWMC) should align itself to deliver space weather information in an internationally agreed-upon standardized format as defined by the aviation user requirements, and be given the mandate to assist the aviation sector in fulfilling the ICAO recommendations.
- The Egyptian Civil Aviation Authority (ECAA) should define a minimum set of requirements for incorporating space weather into operational training for Air Traffic Controllers (ATC), aircrew (pilots and cabin crew), dispatchers, meteorologists, and engineers.
- The Egyptian Civil Aviation Authority (ECAA) should mandate that space weather Information be received by aviation operators and be included as part of their planning and briefing process. This information must meet a minimum set of standards.
- An annual assessment should be carried out of the service performance within the aviation Sector based on space weather events. These recommendations come from an understanding and awareness of the potential impacts of space weather on the aviation sector.

REFERENCE

1. Bom.gov.au. (2019). Space Weather Services website. [online] Available at: https://www.sws.bom.gov.au/.
2. Boroev, R. and Vasiliev, M. (2020a). RELATIONSHIP OF THE ASY-H INDEX WITH INTERPLANETARY MEDIUM PARAMETERS AND AURORAL ACTIVITY IN MAGNETIC STORM MAIN PHASES DURING CIR AND ICME EVENTS. Solar-Terrestrial Physics, 6(1), pp.35–40. doi:10.12737/stp-61202004.
3. Boroev, R. and Vasiliev, M. (2020b). RELATIONSHIP OF THE ASY-H INDEX WITH INTERPLANETARY MEDIUM PARAMETERS AND AURORAL ACTIVITY IN MAGNETIC STORM MAIN PHASES DURING CIR AND ICME EVENTS. Solar-Terrestrial Physics, 6(1), pp.35–40. doi:10.12737/stp-61202004.
4. Borovsky, J.E. and Shprits, Y.Y. (2017a). Is theDst Index Sufficient to Define All Geospace Storms?. Journal of Geophysical Research: Space Physics, 122(11). doi:10.1002/2017ja024679.

5. Cai, X., Burns, A.G., Wang, W., Qian, L., Solomon, S.C., Eastes, R.W., McClintock, W.E. and Laskar, F.I. (2021). Investigation of a Neutral 'Tongue' Observed by GOLD During the Geomagnetic Storm on May 11, 2019. Journal of Geophysical Research: Space Physics, 126(6). doi:10.1029/2020ja028817.
6. Clette, F., Cliver, E.W., Lefèvre, L., Svalgaard, L. and Vaquero, J.M. (2015). Revision of the Sunspot Number(s). Space Weather, 13(9), pp.529–530. doi:10.1002/2015sw001264.
7. Davis, T.N. and Sugiura, M. (1966). Auroral electrojet activity indexAEand its universal time variations. Journal of Geophysical Research, 71(3), pp.785–801. doi:10.1029/jz071i003p00785.
8. Desai, M. and Shah, S. (2018). Impacts of Intense Geomagnetic Storms on NavIC / IRNSS System. Annals of Geophysics, 61(5). doi:10.4401/ag-7856.
9. Filjar, R. (2007). A Study Of Direct Severe Space Weather Effects On GPS Ionospheric Delay. Journal of Navigation, 61(1), pp. 115–128. doi:10.1017/s03734633070044 20.
10. Fisher, G. and Kunches, J. (2011). Building resilience of the Global Positioning System to space weather. Space Weather, 9 (12), p.n/a-n/a. doi:10.1029/2011sw000718.
11. Gonzalez, W.D., Joselyn, J.A., Kamide, Y., Kroehl, H.W., Rostoker, G., Tsurutani, B.T. and Vasyliunas, V.M. (1994). What is a geomagnetic storm? Journal of Geophysical Research, 99 (A4), p.5771. doi:10.1029/93ja02867.
12. Gonzalez, W.D., Tsurutani, B.T. and Clúa de Gonzalez, A.L. (1999). Space Science Reviews, 88(3/4), pp.529–562. doi:10.1023/a:1005160129098.
13. Guo, Y., Li, M., He, S., Xin, P. and Tao, L. (2012). Analysis of the Sun Transit Outage Impact on the Inter-satellite Link of the Navigation Satellite. Lecture Notes in Electrical Engineering, pp.133–143. doi:10.1007/978-3-642-29175-3_13.
14. Joshua, B.W., Adeniyi, J.O., Oladipo, O.A., Doherty, P.H., Adimula, I.A., Olawepo, A.O. and Adebiyi, S.J. (2018). Simultaneous response of NmF2 and GPS-TEC to storm events at Ilorin. Advances in Space Research, 61(12), pp.2904–2913. doi:10.1016/j.asr.2018.03.031.
15. Joshua, B.W., Adeniyi, J.O., Reinisch, B.W., Adimula, I.A., Olawepo, A.O., Oladipo, O.A. and Adebiyi, S.J. (2014). The response of the ionosphere over Ilorin to some geomagnetic storms. Advances in Space Research, 54(11), pp.2224–2235. doi:10.1016/j.asr.2014.08.027.
16. kejian1.cmatc.cn. (n.d.). Space Weather Impacts on Aviation. [online] Available at: http://kejian1.cmatc.cn/vod/comet/spaceweather/aviation_space_wx/print.htm.
17. Kyoto-u.ac.jp. (2022). WDC for Geomagnetism, Kyoto. [online] Available at: https://wdc.kugi.kyoto-u.ac.jp/.
18. Liu, L., Wan, W., Zhang, M.-L., Zhao, B. and Ning, B. (2008). Prestorm enhancements in NmF2and total electron content at low latitudes. Journal of Geophysical Research: Space Physics, 113(A2), p.n/a-n/a. doi:10.1029/2007ja012832.
19. Matzka, J., Stolle, C., Yamazaki, Y., Bronkalla, O. and Morschhauser, A. (2021). The Geomagnetic Kp Index and Derived Indices of Geomagnetic Activity. Space Weather, 19(5). doi:10.1029/2020sw002641.
20. Mendillo, M. (2006). Storms in the ionosphere: Patterns and processes for total electron content. Reviews of Geophysics, 44(4). doi:10.1029/2005rg000193.
21. Mengistu Tsidu, G. and Abraha, G. (2014). Moderate geomagnetic storms of January 22–25, 2012 and their influences on the wave components in ionosphere and upper stratosphere- mesosphere regions. Advances in Space Research, 54(9), pp.1793–1812. doi:10.1016/j.asr.2014.07.029.
22. Penza, V., Berrilli, F., Bertello, L., Cantoresi, M. and Criscuoli, S. (2021). Prediction of Sunspot and Plage Coverage for Solar Cycle 25. The Astrophysical Journal Letters, 922(1), p.L12. doi:10.3847/2041-8213/ac3663.
23. S. O. Ikubanni, S. J. Adebiyi, B. O. Adebesin, O. S. Bolaji, B. J. Adekoya, B. W. Joshua and J. O. Adeniyi (2020). Plasma re-distribution in the African low-latitude ionosphere during intense geomagnetic storms. Journal of the

Nigerian Society of Physical Sciences, pp.228–240. doi:10.46481/jnsps.2020.112.

24. Samed Inyurt (2020). Investigation of Ionospheric Variations During Magnetic Storm Over Turkey. Geomagnetism and Aeronomy, 60(1), pp.131–135. doi:10.1134/s0016793220010120.
25. Space Weather effects on airline operations (Captain Bryn Jones, VAA Cosmic Radiation Project Manager). (n.d.). [online] Available at: https://www.mssl.ucl.ac.uk/cosrad/Website/Publications/SpaceWeatherAL1.pdf.
26. Thales Group. (n.d.). Egypt. [online] Available at: https://www.thalesgroup.com/en/countries/middle-east-africa/egypt [Accessed 6 Aug. 2022].
27. Tsurutani, B.T., Verkhoglyadova, O.P., Mannucci, A.J., Saito, A., Araki, T., Yumoto, K., Tsuda, T., Abdu, M.A., Sobral, J.H.A., Gonzalez, W.D., McCreadie, H., Lakhina, G.S. and Vasyliūnas,
28. V.M. (2008). Prompt penetration electric fields (PPEFs) and their ionospheric effects during the great magnetic storm of 30-31 October 2003. Journal of Geophysical Research: Space Physics, 113(A5), p.n/a-n/a. doi:10.1029/2007ja012879. www.ngdc.noaa.gov. (n.d.). Index of /stp/space-weather/solar-data/solar-indices/sunspot- numbers/group. [online] Available at: http://www.ngdc.noaa.gov/stp/space- weather/solar-data/solar-indices/sunspot- numbers/group/. www.sidc.be. (n.d.). SILSO | World Data Center for the production, preservation and dissemination of the international sunspot number. [online] Available at: http://sidc.be/silso/home. www.spaceweatherlive.com. (n.d.). StackPath. [online] Available at: https://www.spaceweatherlive.com/..
29. Yu, T., Wang, W., Ren, Z., Yue, J., Yue, X. and He, M. (2021). Middle‐Low Latitude Neutral Composition and Temperature Responses to the 20 and 21 November 2003 Superstorm From GUVI Dayside Limb Measurements. Journal of Geophysical Research: Space Physics, 126(8). doi:10.1029/2020ja028427.